Endocrinology, 2023, **164**, 1–14
https://doi.org/10.1210/endocr/bqad007
Advance access publication 23 January 2023
Research Article

Chronic Exposure to Low Levels of Parabens Increases Mammary Cancer Growth and Metastasis in Mice

Jason H. Tong,[1] Sarah Elmore,[1] Shenq-Shyang Huang,[1] Phum Tachachartvanich,[1,2] Katherine Manz,[3] Kurt Pennell,[3] Machelle D. Wilson,[4] Alexander Borowsky,[5] and Michele A. La Merrill[1]

[1]Department of Environmental Toxicology, University of California at Davis, Davis, CA 95616, USA
[2]Laboratory of Environmental Toxicology, Chulabhorn Research Institute, Bangkok 10210, Thailand
[3]School of Engineering, Brown University, Providence, RI 02912, USA
[4]Department of Public Health Sciences, University of California at Davis, Davis, CA 95616, USA
[5]Department of Pathology and Laboratory Medicine, University of California at Davis, Sacramento, CA 95817, USA

Correspondence: Michele A. La Merrill, PhD, Department of Environmental Toxicology, University of California at Davis, Davis, CA 95616, USA.
Email: mlamerrill@ucdavis.edu.

Abstract

Methylparaben (MP) and propylparaben (PP) are commonly used as food, cosmetic, and drug preservatives. These parabens are detected in the majority of US women and children, bind and activate estrogen receptors (ER), and stimulate mammary tumor cell growth and invasion in vitro. Hemizygous B6.FVB-Tg (MMTV-PyVT)634Mul/LellJ female mice (n = 20/treatment) were exposed to MP or PP at levels within the US Food and Drug Administration's "human acceptable daily intake." These paraben-exposed mice had increased mammary tumor volume compared with control mice ($P < 0.001$) and a 28% and 91% increase in the number of pulmonary metastases per week compared with the control mice, respectively ($P < 0.0001$). MP and PP caused differential expression of 288 and 412 mammary tumor genes, respectively (false discovery rate < 0.05), a subset of which has been associated with human breast cancer metastasis. Molecular docking and luciferase reporter studies affirmed that MP and PP bound and activated human ER, and RNA-sequencing revealed increased ER expression in mammary tumors among paraben-exposed mice. However, ER signaling was not enriched in mammary tumors. Instead, both parabens strongly impaired tumor RNA metabolism (eg, ribosome, spliceosome), as evident from enriched KEGG pathway analysis of differential mammary tumor gene expression common to both paraben treatments (MP, $P < 0.001$; PP, $P < 0.01$). Indeed, mammary tumors from PP-exposed mice had an increased retention of introns ($P < 0.05$). Our data suggest that parabens cause substantial mammary cancer metastasis in mice as a function of their increasing alkyl chain length and highlight the emerging role of aberrant spliceosome activity in breast cancer metastasis.

Key Words: tumor growth, mammary cancer, metastasis, methylparaben, propylparaben, estrogen receptor

Abbreviations: BuP, butylparaben; DE, differential expression; EP, ethylparaben; ER, estrogen receptor; FBS, fetal bovine serum; FDA, US Food and Drug Administration; FDR, false discovery rate; H&E, hematoxylin and eosin; HR, hazard ratio; LBD, ligand binding domain; MIN, mammary intraepithelial neoplasia; MP, methylparaben; PP, propylparaben; TEB, terminal end bud; VEH, vehicle.

Parabens, esters of *P*-hydroxybenzoic acid with various alkyl chain lengths, are commonly used in personal care products, pharmaceuticals, and food as preservatives (1). The US Food and Drug Administration (FDA) reports that methylparaben (MP) and propylparaben (PP) are parabens that are "generally recognized as safe" at 0.1% for each paraben in food (1). Humans are exposed to parabens through ingestion of foods and drugs as well as dermal absorption of personal care products (2, 3). Consequently, parabens have been found in numerous human tissues, including adipose tissue, breast tissue, and tumors (4-7). Recent nationally representative surveys of the US population detected MP in the urine of more than 99% of adults and children and PP in 95% of adults and children (8). There are also notable disparities in exposures to these parabens in the United States, whereby non-Hispanic Black women and adolescents have disproportionately high levels of urinary MP and PP (9, 10). For example, non-Hispanic Black girls had more than twice the urinary parabens as non-Hispanic White girls in the National Health and Nutrition Examination Survey (2003-2008) (9). Given Black women are also more likely to die from breast cancer than white women in the United States (11, 12), the possibility that their excess paraben exposure may cause increased breast cancer mortality merits examination.

Estrogenic action has been supposed as a potential causal link between paraben exposure and breast cancer risk. Given that the majority (75%) of breast cancer cases are estrogen receptor (ER)-positive and total lifetime exposure to estrogen is a breast cancer risk factor, the binding and stimulation of ER-mediated cell proliferation by parabens in the culture of human breast cancer and epithelial cells is concerning (13-17). In addition to their promotion of cell proliferation, parabens have also increased motility and invasive

Received: 9 September 2022. **Editorial Decision:** 10 January 2023. **Corrected and Typeset:** 3 February 2023

activity in human breast cancer cells (18). These in vitro findings highlight that parabens can cause proliferation, invasion, and metastasis, which are hallmarks of cancer (19) and contribute to breast cancer-associated mortality. However other in vitro studies indicate that parabens, especially those with shorter alkyl chains such as MP, are very weak to negligible activators of ER (16, 20-23).

Exposure to parabens could also contribute to breast cancer by stimulating the precancer niche. For example, in vitro (24-26), in vivo (27), and human (28) studies indicate that parabens may cause overweight and obesity, the latter of which is a breast cancer risk factor (29). The increased growth of human breast epithelial cells exposed to MP or PP (15) and effects of exposure to MP during rat puberty on mammary gland structures and cell-cycle regulation (30) suggest that these parabens may also indirectly increase breast cancer risk by targeting the rapidly proliferating pubertal mammary epithelium.

In this study, we investigated whether parabens play a role in tumorigenesis and metastasis through the transcription-mediated effects of ER by promoting obesity and/or by altering puberty using in silico, in vitro, in vivo, and transcriptome approaches. We used a mouse model of mammary cancer pulmonary metastasis. Paraben doses approximated the safe level the US FDA generally recognizes, were within the human acceptable daily intake of parabens proposed by the Food and Agriculture Organization of the United Nations and World Health Organization Joint Expert Committee on Food Additives, and were initiated during puberty given the possible developmental susceptibility associated with known adolescent paraben exposure. Under these exposures, we examined the effect of MP or PP on mammary tumor onset, growth, pathology, and transcriptomes, as well as the rate of pulmonary metastasis colony formation. The binding of 4 parabens to human ER alpha and beta was examined in a high-resolution molecular docking model, and the transactivation of human ER was evaluated for these 4 parabens.

Methods

Reagents

MP (purity ≥99.0%, CAS No. 99-76-3) and PP (purity ≥99.0%, CAS No. 94-13-3) were purchased from Sigma-Aldrich (St. Louis, MO). Organic, extra-virgin olive oil (Spectrum) was used as the solvent for the parabens and as the vehicle (VEH) control. Pure ethanol (89125-172) was purchased from VWR (Radnor, PA).

Thermo Scientific 10% Neutral Buffered Formalin (5725), Fisher Scientific Chloroform (C298-500), Fisher Scientific Permount Mounting Media (SP15-500), Fisher Scientific acetic acid (AC222140025), Invitrogen SuperScript VILO cDNA Synthesis Kit (11754250), and Applied Biosystems PowerSybr Green PCR Master Mix (4367659) were purchased from Thermo Fisher Scientific (Waltham, MA). Sigma-Aldrich Carmine (C1022-5G) and Millipore Xylene (XX0060-4) were purchased from MilliporeSigma (Burlington, MA). Anti-ER-α (clone MC-20, RRID: AB_631470) was purchased from Santa Cruz Biotechnology (Dallas, TX). DNase I (M0303S) was purchased from New England BioLabs (Ipswich, MA). AllPrep DNA/RNA/Protein Mini Kit (80004) was purchased from Qiagen (Germantown, MD). Sigma-Aldrich Serum Triglyceride Determination Kit (TR0100) was purchased from MilliporeSigma and the NEFA-HR(2) kit was purchased from Wako (Richmond, VA). EnVision FLEX Wash Buffer and 3,3′-diaminobenzidine solution were purchased from Agilent (Santa Cruz, CA). VECTASTAIN Elite ABC HRP Kit (PK-6100, RRID: AB_2336819), anti-rabbit (K4003, RRID: AB_2630375), and anti-rat IgG (BA-9400, RRID: AB_2336202, and BA-9401, RRID: AB_2336208) were purchased from VectorLabs (Newark, CA). ClearMount was purchased from American MasterTech Scientific (Lodi, CA).

Mice

Hemizygous mice born from female C57BL/6J mice and male B6.FVB-Tg(MMTV-PyVT)634Mul/LellJ mice (Jackson Laboratory, Bar Harbor, ME) were randomly enrolled in treatment groups (n = 20 mice/treatment; Supplementary Fig. S1) (31). The PyVT oncogene model of spontaneous mammary tumors forms ER-positive neoplasms that progress to malignancies (32, 33). PyVT has been used extensively to model human breast cancer because of its overlap with human breast cancer activation pathways (34, 35). Its complete backcross to the C57BL/6J background develops neoplasms progressing to malignancies with the same pathway activation, whereas the host genetics delays initiation and progression (36). Our sample size of 20 mice per treatment was selected based on a previous study of lung metastasis in these mice (37). Remaining hemizygous female littermates were euthanized at postnatal day 49 (herein called "late puberty," n = 7 mice/MP or VEH treatment). Insufficient additional hemizygous females were available to sufficiently power the inclusion of PP treatment in this late puberty terminal analysis (38). Wild-type female littermates were evaluated for paraben levels (n = 3 mice/VEH, MP, or PP treatment). MP and PP were dissolved in absolute ethanol (1.0 g paraben/mL), which was diluted in organic, extra-virgin olive oil to 20 mg paraben/mL. Mice were orally gavaged daily with VEH (5 mL/kg body weight) or 100 mg MP or PP/kg body weight from weaning at postnatal day 28 until euthanasia.

Mammary glands were palpated to record tumor onset, and once palpable, tumors were measured with digital calipers (Mitutoyo, Aurora, IL) 3 times weekly. Tumor volumes were estimated as one-half the product of the greatest tumor diameter and the square of the lesser tumor diameter. Mice were euthanized when the combined volume of subcutaneous tumors was found in excess of 4 cm^3. No mice became moribund, lost > 20% of their pretumor body mass, or had ulcerated or necrotic tumors. Mice had access to food (3.07 kcal/g; 5053, LabDiet, St. Louis, MO) and water ad libitum. All animal procedures and protocols were approved by UC Davis' Institutional Animal Care and Use Committee.

Metabolic Phenotyping

Fat and lean mass were measured using EchoMRI (100 V, EchoMRI LLC, Houston, TX). Mice were fasted for 5 hours, dosed, and had tail blood collected 1 hour later. Blood pressure was noninvasively measured using the CODA High Throughput System (Kent Scientific, Torrington, CT). Blood glucose was measured using a glucometer (AlphaTRAK 2, Zoetis, NJ). Plasma triglycerides and nonesterified fatty acid levels were measured through absorbance-based enzymatic assays. Rectal temperature was measured by thermocouple probe (RET-4, BAT-12R, Physitemp, Clifton, NJ). The sum of weekly food intake (g) throughout the dosing period was divided by the number of mice that had access and the number

of access days (g/d) and was converted into daily caloric intake (kcal/d).

Histopathology and Immunohistochemistry

Whole lungs and half of each primary mammary tumor from 24- to 26-week-old hemizygous mice were fixed in 10% neutral buffered formalin and stored in 70% ethanol. Mammary tumors were paraffin-embedded and sectioned at a thickness of 5 µm. Routine hematoxylin and eosin (H&E) staining was performed as previously described (39).

Inguinal mammary glands from 7-week-old hemizygous mice (n = 7/VEH and MP treatment) were excised, and previously published methods were used as briefly described here (39, 40). Left (4th) inguinal mammary glands were placed on charged slides and fixed in Carnoy solution overnight. Mammary glands underwent a series of ethanol washes (70%-30% ethanol) before being rinsed in water and stained with carmine aluminum potassium sulfate overnight. The stained glands were rinsed with water and ethanol and were cleared in xylene before whole mounting with Permount media. Right (9th) inguinal mammary glands were cut into 2- to 3-mm slices, subjected to 24 hours of zinc-salt fixation, dehydrated, paraffin-embedded, and sectioned into 4-µm slices. Sections were deparaffinized and rehydrated before ERα antigen retrieval in citrate buffer (10 mM sodium citrate, pH 6). Immunohistochemistry was performed with biotinylated anti-rabbit at 1:1000 in goat serum using the VECTASTAIN Elite ABC kit (Vector Laboratories, Burlingame, CA). This was followed by Mayer hematoxylin counterstaining. Additional 5-µm sections of right (9th) inguinal mammary glands were also subjected to routine H&E staining.

Whole-slide image scanning microscopy was performed with the Leica Aperio AT2 ScanScope and were viewed with eSlideManager software (Leica Biosciences, Vista, CA). ERα-positive cells were counted inForm Cell Analysis software (PerkinElmer, Waltham, MA). The mammary epithelia, mammary intraepithelial neoplasia (MIN), lymph nodes, endothelia, and adipocytes were gated and annotated by QuPath-0.3.2 (41, 42). Terminal end buds (TEBs; late puberty study only) and pulmonary metastasis foci (mouse with palpable mammary tumors only) were counted by 2 individuals. Structures were called TEB when found at the tips of ducts and their widest point was at least twice the width of the contiguous duct (37). All histopathological features (muscle and stroma invasion, and the presence of necrosis, pyknotic cells, TEB, and MIN) were examined by experienced pathologists blinded to treatment groups. Stroma was defined as nonepithelial cells of the mammary gland such as adipocytes and endothelial cells.

RNA Isolation and Sequencing

One-half of the primary mammary tumor was trimmed along its exterior and pulverized while frozen for total RNA extraction using DNase I following the manufacturer's protocol (Qiagen, Germantown, MD). Libraries were 3′ Tag-sequenced using the HiSeq 4000 (Illumina, San Diego, CA). The sequence was aligned with the Ensembl reference genome GRCm38, resulting in ~5 million reads per sample. Primary mammary tumor from 1 mouse in the vehicle control group was lost during RNA extraction, resulting in a sample size of 19 for the vehicle group for RNA sequencing and downstream analyses.

Quantitative RT-PCR

Total RNA was reverse transcribed according to the manufacturer's protocol (Thermofisher Scientific, Waltham, MA). Semiquantitative PCR was using the following primer sequences: *Gata3* forward (5′-TGTCTGCGAACACTGAGCTG-3′) and reverse (5′-CGATCACCTGAGTAGCAAGGA-3′), *Stat3* forward (5′-ACCCAACAGCCGCCGTAG-3′) and reverse (5′-CAGACTGGTTGTTTCCATTCAGAT-3′), *Il6st* forward (5′-CGGCTCATATGGAAGGCACT-3′) and reverse (5′-CCCACCTTGTTTCTTGCTGC-3′), and *Esr1* forward (5′-CCGCAGCTGTCTCCTTTCCT-3′) and reverse (5′CGGTTCTTGTCAATGGTGCA-3′). Fold change of single gene expression was determined with the average Ct from technical triplicates using the delta-delta Ct method with *Actb* forward primer (5′-CTGACAGGATG CAGAAGGAG-3′) and reverse primer (5′-GATAGAGCCAC CAATCCACA-3′).

Chemical Analysis

Submandibular blood was collected 1 hour after treatment, when plasma paraben levels were expected to be highest (43). Plasma samples (3 mice/treatment), 3 method blanks, and 3 recovery spike samples were blindly extracted using liquid chromatography coupled to high-resolution mass spectrometry, similar to as previously described (44). The method blanks comprised 200 µL fetal bovine serum (FBS), whereas the recovery spike samples consisted of 200 µL FBS spiked with 1000 ppb MP and PP. All samples were initially stored at −80 °C and were defrosted at −20 °C until extraction. Each plasma sample and method blank was spiked with 100 µL of 1000 ppb ethylparaben (EP) and butylparaben (BuP) for use as surrogate standards to assess recovery. Targeted analysis of MP, PP, EP, and BuP was performed using a Thermo Liquid Chromatography Orbitrap Q Exactive HF-X mass spectrometer equipped with a Thermo Vanquish UHPLC system.

Molecular Docking

Molecular docking was performed as previously described (45). The crystal protein structures of human ERα (Protein Data Bank ID: 3UUD) and human ERβ (Protein Data Bank ID: 2YLY) were used as initial conformations for molecular docking in the Protein Preparation Wizard in Maestro and tools therein (Schrödinger Release 2018-4: Maestro, Schrödinger, LLC). Before the molecular docking using induced fit with glide, hydrogen atoms were removed, and the protein structures were minimized to reduce steric clashes using the OPLS_2005 force field. To generate the best molecular geometry with the lowest energy level, all paraben structures and endogenous ligand (ERs: 17β-estradiol) were minimized using MacroModel. Parabens and endogenous ligand were then docked into the ligand binding domain (LBD) of the 2 hormone receptors. A total of 15 poses were generated for each protein structure and evaluated by docking score.

Cell Culture

The human mammary adenocarcinoma MCF7-derived VM7Luc4E2 cells (formerly BG1Luc4E2), stably transfected with a human ER-responsive luciferase reporter gene, were used for the experiment and cultured according to the procedure described previously (46). To minimize interferences from

other steroids, cells were expanded to confluence under the steroid hormones-deprived condition composed of phenol red-free DMEM (Gibco, Grand Island, NY) supplemented with 10% charcoal stripped FBS (Gibco). Cells were treated in triplicate with either 1 nM 17β-estradiol (E2), 1 μM EP, 10 μM EP, 1 μM MP, 10 μM MP, 1 μM PP, 10 μM PP, 1 μM BuP, 10 μM BuP, or 1% v/v dimethyl sulfoxide (vehicle control). After 24 hours' incubation, cells were washed with PBS and lysed for 15 minutes. Luciferin reagent was injected into each well and the relative light units were measured using a luminometer (M200Pro, Tecan, Männedorf, Switzerland). The relative light units from each treatment (E2, MP, EP, PP, and BuP) were normalized to the vehicle control.

Data Analyses

Outcomes were tested for normality and transformed into normal distributions for regression analyses as needed. We modeled time to tumor presence using PROC PHREG (SAS Enterprise Guide 7.1, Cary, NC). We modeled time to vaginal opening with proportional hazards regression using left censoring to account for treatments beginning at PND21 (PROC ICPHREG). We modeled the rate of pulmonary metastasis using a Poisson distribution and log link function to calculate hazard ratios (HRs) accounting for the number of days with mammary tumors and counter (PROC GENMOD). We modeled the rate of muscle invasion using a Poisson distribution and log link function to calculate HRs among H&E slides that included skeletal muscle (VEH, n = 8; MP, n = 11; PP, n = 10). Log-transformed total tumor volume was modeled with days since first palpable tumor as an independent term accounting for repeated measures per mouse (PROC MIXED). Body mass was modeled with and without total tumor volume as an independent model term and analyzed per week accounting for repeated measures per mouse (PROC MIXED). Differences in TEB numbers between MP and VEH were modeled independent of blinded counters (PROC MIXED). Body temperature and blood pressure were modeled using linear regression accounting for repeated measures per mouse (PROC MIXED). Tissue weights, fat and lean mass, caloric intake, blood metabolic parameters, luciferase, and single gene expression were evaluated using general linear models (PROC GLM). Data were graphed using Prism (GraphPad, San Diego, CA).

Differential expression (DE) analyses of RNA-sequencing data were adjusted for a false discovery rate (FDR) < 0.05 using the voom function in the limma software package (47) of R (version 3.4.4) and visualized (Morpheus). KEGG Pathway Database (version as of 11/4/2019) data (48) were extracted and Wilcoxon rank-sum tests identified pathway enrichment within our dataset by testing that *P* values from DE analysis for genes in the pathway were smaller than those not in the pathway using the KEGGREST (version 1.18.1) R Bioconductor package (49). Log-fold changes of genes were mapped onto KEGG pathways using the Pathview (version 1.18.2) Bioconductor package (50).

Results

Paraben Exposures are Relevant to the Human Condition

The paraben exposures were designed to be relevant to humans such that oral daily dose of 100 mg parabens/kg was a human equivalent dose of 8.31 mg/kg body weight, a concentration within the human acceptable daily intake of 0 to 10 mg parabens per kg body weight (51-54). We further compared our oral daily dose of 100-mg parabens/kg with the FDA "generally recognized as safe" level of 0.1% for each paraben in food by accounting for the measured ranges of food and body mass of our mice (1). The mice in the study had paraben food intakes in the range of 0.05% to 0.13% (mg paraben/mg food and olive oil vehicle) with the median body weight mice having a food intake equivalent to the FDA "generally recognized as safe" level of 0.1% (Table 1).

To determine the internal dose of parabens after chronic exposure, C57BL/6J female mice were exposed to vehicle, MP, or PP for 83 to 85 days. Despite that mice were dosed with 100-mg MP or PP/kg body weight, MP levels in plasma were nearly 15-fold higher than PP levels in plasma; 1 hour after the final oral exposure, the median paraben concentrations found in the plasma of C57BL/6J mice were 9969.88-ng MP/mL plasma among the MP treatment group, and 675.51-ng PP/mL plasma among the PP treatment group (Supplementary Table S1) (31). No MP was detected in the PP treatment group, and no PP was detected in the MP treatment group, but a small amount of MP (3.16 ng MP/mL plasma) was detected among the VEH treatment group (Supplementary Table S1) (31).

Parabens Increase Mammary Tumor Growth and Metastasis

The timing of palpable tumor onset (MP vs VEH: HR = 1.0; 95% CI, 0.6- 1.9; PP vs VEH: HR = 1.2; 95% CI, 0.7-2.0) did not significantly differ across treatment groups (Fig. 1A-B). There was a qualitative increase in the tumor cell invasion of local skeletal muscle and stroma tissue among paraben-treated mice that did not reach statistical significance (Fig. 1A, Supplementary Table S2) (31). There was also a qualitative decrease in the presence of necrosis and minimally invasive neoplasms among paraben-treated mice that did not reach statistical significance (Fig. 1A, Supplementary Table S2) (31). The multiplicity of mammary tumors was also unchanged by treatment (Supplementary Fig. S2A) (31).

However, paraben exposure caused cancer phenotypes associated with advanced pathologic stage in human breast cancers, namely increased growth and distant invasion. MP and PP exposure caused a significant increase in total mammary tumor volume over time (MP vs VEH, $P < 0.001$; PP vs VEH, $P < 0.0001$; Fig. 1C). Pathological examination of mammary tumor metastasis presenting as pulmonary tumors revealed that mice chronically exposed to "human acceptable daily intake" doses of MP or PP had a 28% or 91% increase in the number of pulmonary metastases per week, relative to mice exposed to the vehicle control, respectively (MP vs VEH, HR = 1.3; 95% CI, 1.2-1.4; $P < 0.0001$; PP vs VEH, HR = 1.9; 95% CI, 1.8-2.1; $P < 0.0001$; Fig. 1D). This did not result in a significantly greater multiplicity of pulmonary metastasis (Supplementary Fig. S2B) (31).

Paraben Effects on Body Composition are Inconsistent With Cancer Risk

Because it has been previously suggested that parabens cause obesity and obesity is a breast cancer risk factor (27-29), we examined body composition as a possible explanation of the tumor virulence observed. Hemizygous mice with paraben exposure had higher body weights compared with controls

Table 1. Percentile body weights of paraben-exposed mice and their food intakes to illustrate range of paraben concentrations in diet

Body weight rank (percentile)	Body weight (g)	Oil volume dosed (μL)	Oil mass dosed (mg)	Measured food intake (g)	Paraben mass dosed[a] (mg)	Equivalent paraben oral intake (%/d)[b]
0	12.90	64.50	59.08	2.24	1.29^{P}	0.06
25	18.30	91.50	83.81	2.44	1.83^{M}	0.07
50	20.00	100.00	91.60	1.85	2.00^{M}	0.10
75	21.40	107.00	98.01	1.95	2.14^{P}	0.10
100	28.30	141.50	129.61	2.13	2.83^{M}	0.13

Body weight and body weight ranks included only paraben exposed mice (n = 40).
[a]Concentration of MP (^{M}) and PP (^{P}) in oil were both 20-mg paraben/mL oil.
[b]Equivalent paraben oral intake = (paraben, mg)/(vehicle oil and food, mg) × 100%.

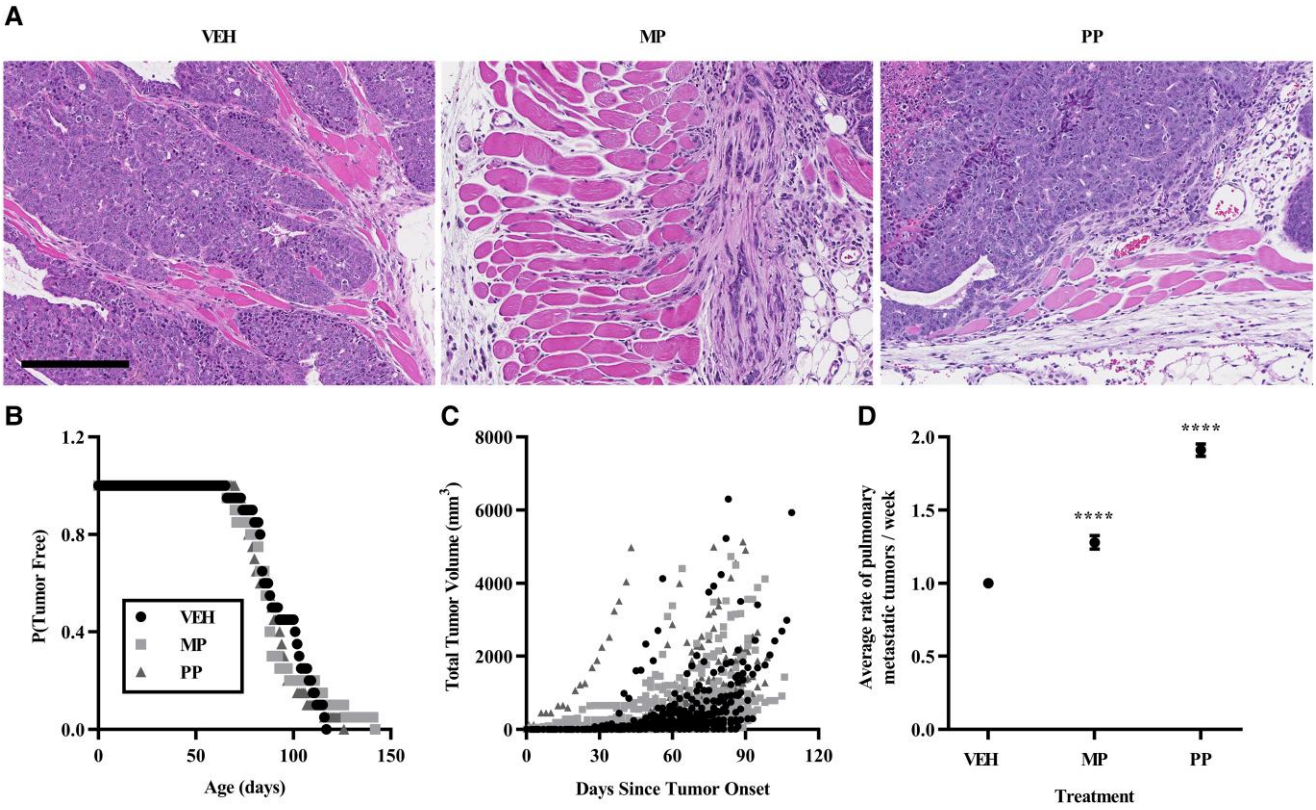

Figure 1. Parabens and mammary tumor metastasis. (A) Images of local invasion of muscle in hematoxylin and eosin-stained primary mammary tumors of 24- to 25-week-old mice exposed to vehicle control, methylparaben, or propylparaben. Bar measures 200 μM. (B, C) Tumor onset and tumor growth were evaluated by palpation and digital calipers, respectively. (D) Effects of treatment exposure on rate of pulmonary metastases represented by hazard ratios. $^{****}P < 0.0001$ with mean and standard error graphed for 20 mice/treatment.

(Supplementary Fig. S3A) (31). This could not be solely explained by mammary tumor mass given that the positive effect of parabens on body weight was only partially attenuated when body weight was adjusted for tumor volume (Supplementary Fig. S3B) (31). However, whole-body and tissue-specific fat mass did not significantly differ between treatment groups (Supplementary Fig. S3C-D, Supplementary Table S3) (31). Although PP-exposed mice had significantly more lean mass compared with the VEH-exposed mice at 13 weeks of age (Supplementary Fig. S3E) (31), this trend was not seen at a later timepoint of 21 weeks of age and was not significant relative to body mass (Supplementary Fig. S3F) (31). Additionally, energy balance, assessed by caloric intake and rectal temperature, did not appear to differ between treatments (Supplementary Fig. S4A-B) (31). Further, paraben exposure had no statistically significant effect on metabolic blood parameters (eg, blood pressure, glucose, insulin, triglyceride, and nonesterified fatty acids) (Supplementary Figure S4C-F) (31).

MP Doubled Terminal end Buds of Mammary Glands During Late Puberty

Given the known relationship between puberty timing and mammary cancer risk, we evaluated puberty in an analysis of hemizygous female mice that were in excess of those needed

for the tumor studies. Hemizygous MP-exposed mice reached vaginal opening at the same rate as VEH-exposed mice (Supplementary Fig. S5A) (31). The mammary glands of 7-week-old hemizygous mice exposed to MP had more than twice the number of TEBs compared with mice exposed to the vehicle control ($P < 0.01$; Supplementary Fig. S5B-D) (31). Microscopically, the relative abundance of epithelial cells, adipocytes, and MIN did not differ between MP- and VEH-exposed 7-week-old hemizygous mice (Supplementary Fig. S6A-D) (31). The nuclear area and perimeter of epithelial cells and MIN was also not significantly different across VEH and MP (Supplementary Fig. S6E-G) (31). Similarly, there was no evidence that MP altered ER expression or uterine weight when hemizygous mice were 7 weeks old (Supplementary Fig. S7; Supplementary Table S3) (31).

Parabens Bind and Activate Human Estrogen Receptors

To investigate the effect of paraben alkyl chain length on the binding affinity of parabens at human ERs (55), we examined atomic-level interactions between parabens and amino acid residues within the LBDs of human ERα and ERβ using molecular docking. The lowest docking scores were observed for the molecular docking of endogenous ligands (Fig. 2; Supplementary Table S4) (31), indicating endogenous ligands had the greatest affinity to their receptors and validating our molecular docking approach. The docking scores was relatively similar across parabens and both ERs (eg, from—7.4 to—6.8 in ERs) (Figure 2; Supplementary Table S4) (31). In the ER LBDs, hydrogen-bonding and Pi-Pi stacking interactions appeared to be the major chemical interactions stabilizing the binding between parabens and ERs for both receptor subtypes (Fig. 2C-F). The hydroxyl group on the aromatic rings of all parabens formed the hydrogen bond with the key amino acid residues in ERα (Glu353, Arg394) and ERβ (Glu305, Asp303, and Trp335). The phenyl ring of parabens was stacked with the aromatic side chain of the Phe or Trp residues in both ER subtypes (Phe404 for ERα and Phe356 or Trp335 for ERβ). In addition, Ile and Leu residues were found to be in the proximity with the alkyl chain of parabens that stabilized the binding of parabens and amino acid residues through hydrophobic interaction.

Because molecular docking represents predicted binding affinities and binding affinities are not the same as receptor activity, we performed a luciferase reporter gene assay for human ER. All tested parabens increased estrogenic activity (Fig. 3). Despite little difference in the docking scores of parabens, there was a clear positive relationship between alkyl chain length and ER activity of parabens at the 10-μM dose (Fig. 3A). ER transactivation increased as the alkyl chain length of parabens increased (Fig. 3B).

Parabens Perturb RNA Metabolism in Mammary Tumors

Given ER is a transcription factor activated by parabens, we examined the primary mammary tumor transcriptome using 3′ Tag-sequencing. We mapped 7622 unique genes that underwent DE and KEGG pathway enrichment analyses. There were 288 and 412 DE genes in primary mammary tumors of mice exposed to MP or PP compared with the VEH control group, respectively; 158 of those DE genes were common to both MP and PP (FDR < 0.05; Fig. 4A-B; Supplementary Table S5) (31). Further, the increased expression of subset of those DE genes that are expressed in human luminal breast cancer and metastasis (56, 57) (eg, *Esr1* also known as ERα, *Gata3*, *Il6st*, *Stat3*) by paraben exposure was validated using quantitative PCR (Fig. 4C).

To evaluate whether parabens contributed to distinct mammary tumor functions, we conducted pathway analysis. There were 44 and 40 significantly enriched KEGG pathways among MP- or PP-exposed mice, relative to the control group, respectively (Fig. 4D-E; Supplementary Table S6) (31). When the enriched KEGG pathways were ranked by significance, the top 3 pathways common to both parabens were the cell cycle (MP, $P < 0.0001$; PP, $P < 0.001$), the ribosome (MP, $P < 0.001$; PP, $P < 0.00000001$), and the spliceosome (MP, $P < 0.001$; PP, $P < 0.01$; Fig. 5A-C). Nearly all of the individual genes enriching these pathways had the same direction of expression change in both MP- and PP-exposed mammary tumors relative to the vehicle control. For example, paraben exposure decreased expression of RNA encoding nearly all ribosomal proteins with a notable absence of increased expression of RNA encoding ribosomal proteins by either paraben (Fig. 5B). Similarly, paraben exposure decreased expression of RNA encoding nearly all spliceosome components (Fig. 5C). Only 1 gene, *Hsp73*, was upregulated in the spliceosome by exposure to the parabens (Fig. 5C). Although ER signaling is associated with proliferation, the expression of canonical targets of ER in the cell-cycle pathway were not strongly influenced by paraben exposure; for example, neither paraben increased expression of *c-Myc* or *Cyclin D1* (Fig. 5A). Despite the increased *Esr1* expression in paraben-exposed mammary tumors, the estrogen-signaling KEGG pathway was not enriched in paraben-exposed mammary tumors.

We next investigated whether paraben treatment had a functional consequence on the mammary tumor spliceosome by evaluating the presence of intronic RNA and its differential expression with respect to exposure to either paraben compared to vehicle control. Although we did not detect any increased intron expression in mammary tumors from MP-exposed mice compared with vehicle control exposed mice, 20 genes from mice exposed to PP had significantly different intron content compared with vehicle-exposed mice (FDR < 0.05; Fig. 5D; Supplementary Table S7) (31). PP exposure was associated with decreased intron retention in *Fads2*, *Kifc5b*, and *Degs1*, the top 3 most differentially expressed introns in PP-exposed mammary tumors compared with controls (Fig. 5D). We proceeded to evaluate whether introns retained differentially with respect to PP exposure occurred among coding mRNA also differentially expressed with respect to PP exposure. Ten of the 20 genes (50%; *Arhgef6*, *Vav3*, *Peli2*, *Man2a1*, *Apol6*, *Cltb*, *Camk2d*, *Col14a1*, *Irs1*, *Col8a1*) with differentially expressed intronic RNA were also DE mRNA in PP-exposed mammary tumors compared with vehicle-exposed mammary tumors.

Discussion

Parabens are in widespread use in the United States and those parabens that are generally recognized as safe by the US FDA, MP and PP, are found in nearly all (≥95%) US adults and children. The relevance of MP toxicity to human health is underscored by the fact that MP was the most common and abundant paraben measured in human breast tumor samples and in the urine of women and girls of a US representative

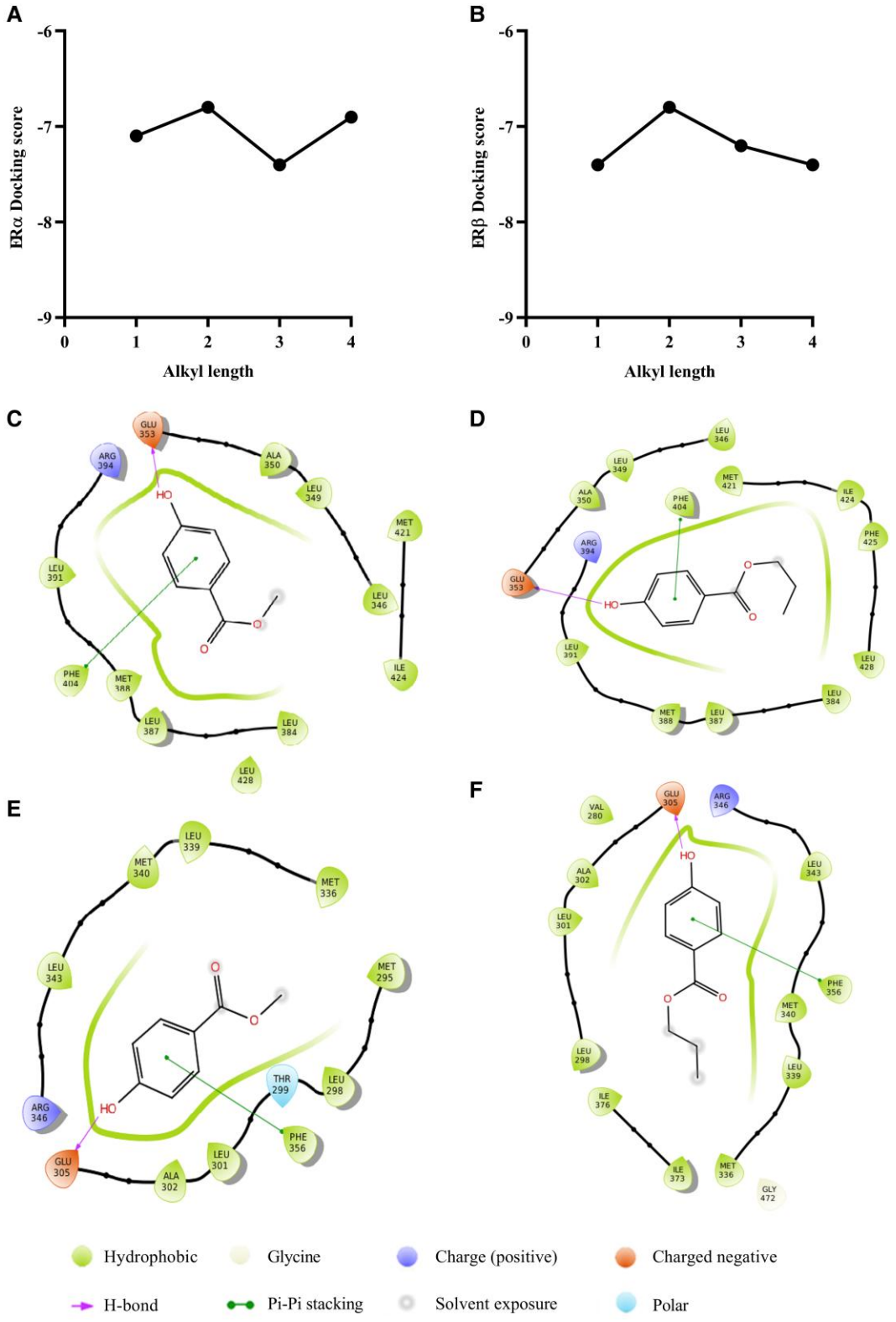

Figure 2. Parabens and estrogen receptors. (*A*) Estrogen receptor (ER)α and (*B*) ERβ docking scores of parabens differing in alkyl chain length using in silico using induced fit with glide; 1 = methylparaben (MP), 2 = ethylparaben, 3 = propylparaben (PP), and 4 = butylparaben. (*C-F*) Predicted molecular interaction between parabens and steroid receptor ligand-binding domains. (*C*) MP and ERα, (*D*) PP and ERα, (*E*) MP and ERβ, and (*F*) PP and ERβ predicted molecular interactions.

sample (8, 20). Here, we demonstrated that female mice administered either MP or PP at levels relevant to human exposures had increased rates of mammary tumor growth and pulmonary metastasis. In support of parabens as estrogenic chemicals, parabens bound human ER alpha and beta in a high-resolution molecular docking model, human ER

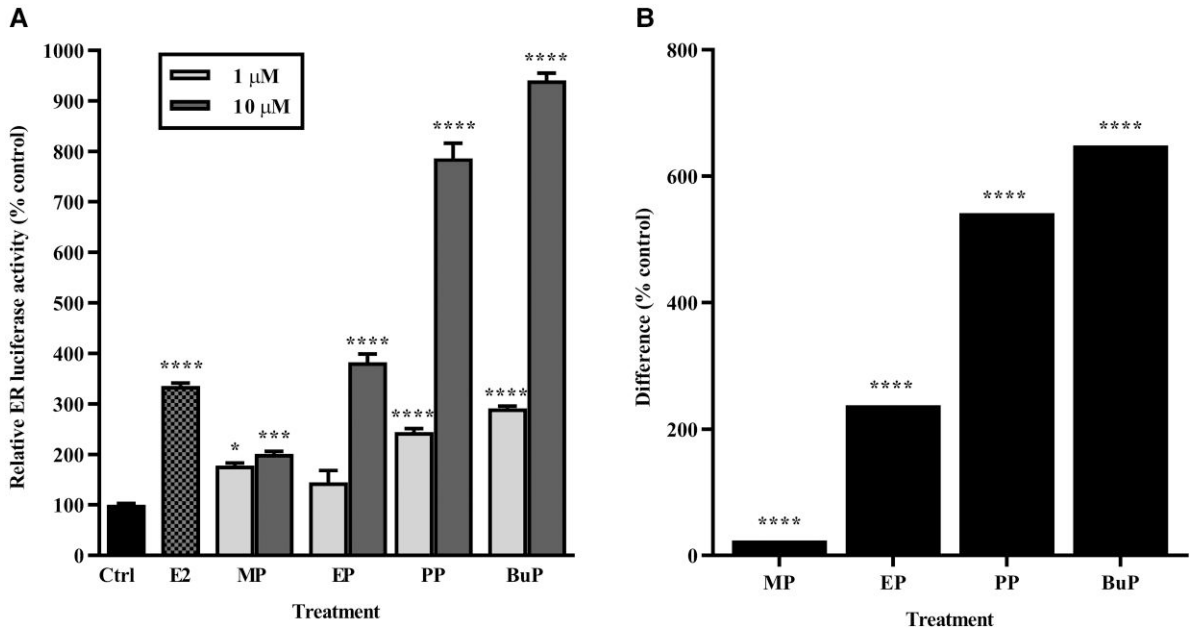

Figure 3. Estrogenic activity and alkyl chain length of parabens. (*A*) Estrogenic activity was measured by a luciferase reporter gene assay in human breast carcinoma Vm7LucE2 cells relative to dimethyl sulfoxide (DMSO) control. (*B*) Difference in activity between treatment groups relative to DMSO control. BuP, butylparaben; Ctrl, DMSO; E2, 1 nM estradiol; EP, ethylparaben; MP, methylparaben; PP, propylparaben. $^{*}P < 0.05$, $^{***}P < 0.001$, $^{****}P < 0.0001$ relative to DMSO control with mean and standard error graphed for n = 3/treatment.

transactivation was directly proportional to paraben alkyl chain length, MP increased TEB abundance during late puberty, and mammary tumors from mice exposed to parabens were enriched with ER expression. However, the estrogenic effects of parabens in vivo were not evident in assessments of vaginal opening timing or pathway analysis of the mammary tumor transcriptome. Instead, unsupervised transcriptome analysis identified a novel mechanism of parabens targeting RNA metabolism that included excess intron retention in mammary tumors. The accelerated mammary tumor growth by parabens could have been caused by several interrelated phenomena in mammary tumors, including excess ER expression and activation as well as changes in RNA metabolism and cell-cycle progression.

Exposure to MP or PP increased the mammary tumor growth rate, similar to the increased tumor volume reported in mice exposed to MP in 2 human breast cancer xenograft models (22). These in vivo results are consistent with extensive in vitro studies demonstrating parabens have one of the key characteristics of carcinogens (eg, "alter cell proliferation, cell death, or nutrient supply") used by the World Health Organization's International Agency for Research on Cancer to identify carcinogens (58). For example, MP and PP exposures increased growth of human breast cancer cell lines, with greater potency of PP compared with MP in studies that examined both parabens (16, 20). Further, during late puberty, mice exposed to MP had delayed regression of TEB, which may be an indicator of increased tumor initiation risk given this rapidly proliferating structure is considered to have heightened sensitivity to carcinogens (38). This heightened sensitivity of the paraben-exposed TEB may be furthered by the increased growth and proliferation of mammary epithelial cells from both humans and mice exposed to parabens in other studies (15, 22, 59, 60).

We are unaware of other studies that may have examined mammary tumor metastasis from paraben exposure in vivo. However, human breast cancer cells in vitro had enhanced motility and invasion when exposed to concentrations of PP relevant to humans (18, 61). As we observed with potency between parabens in mice and human ER transactivation, MP was a less potent in vitro stimulator of human breast tumor cell motility and invasion than was PP (18, 61). Further, indirect evidence supports the significant effects of MP on mammary tumor metastasis, where significant gene expression changes in mammary glands of rats exposed to MP were also significantly associated with breast cancer mortality in a human population-based cohort (62). Collectively, these data across 3 mammalian species support a role of paraben exposure in mammary cancer metastasis.

Mammary tumor ER expression was elevated by parabens, consistent with another study of parabens as well as the luminal breast cancer subtype that composes the majority of human breast cancers and frequently metastasizes (16, 56). Parabens bound and activated human ER, and elsewhere parabens stimulated ER-mediated proliferation of human cancer cells (16, 63). Hence, elevated ER expression and activation could explain the increased mammary tumor growth in paraben-exposed mice.

ER expression can also facilitate the metastatic cascade from local invasion to tumor growth at metastatic sites (64), consistent with MP and especially PP increasing human breast cancer cell invasion in vitro (18) and mammary cancer metastasis in vivo here. However, the positive relationship between paraben alkyl chain length and human ER activation did not extend to molecular docking analysis of the human ER LBD here or by others (16, 23). It is unlikely that species differences explain the discrepancy of in silico human ER docking with in vitro human ER reporter assays and in vivo mouse phenotypes given the high homology between human and mouse ERα

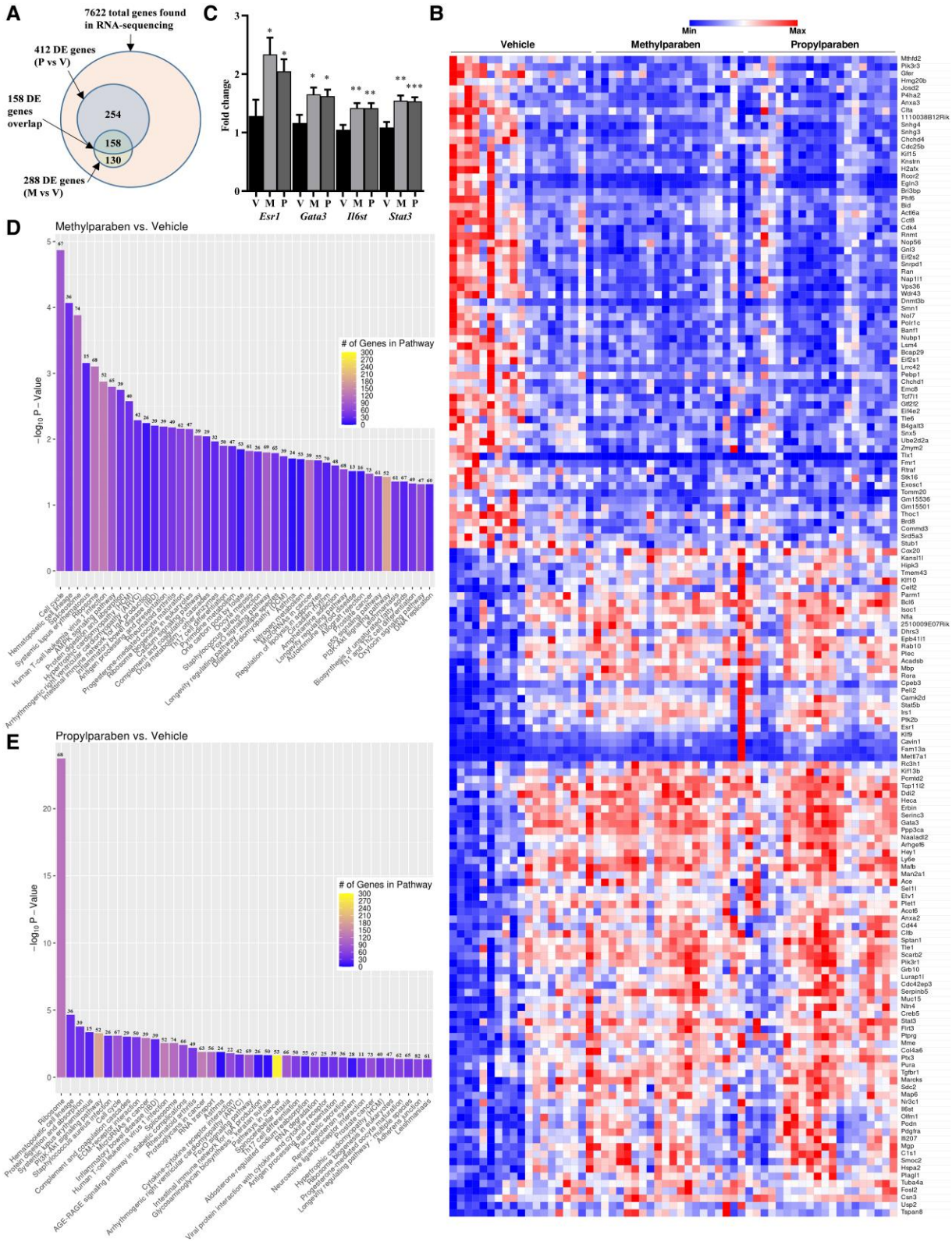

Figure 4. Gene expression and biological pathways in primary mammary tumors. (*A*) Venn diagram of total transcripts and differentially expressed (DE) genes between methylparaben (M) or propylparaben (P) exposure relative to the vehicle (V) control in primary mammary tumors from PyMT hemizygous female mice detected by 3′ Tag-seq. (*B*) Heat map of log-fold change for the 158 DE genes common to primary mammary tumors from treated PyMT hemizygous female mice using 3′ Tag-seq. (*C*) Fold change in expression of *Esr1*, *Gata3*, *Il6st*, and *Stat3* relative to *Actb* in primary mammary tumors of PyMT hemizygous female mice exposed to VEH, MP, or PP through quantitative RT-PCR. (*D-E*) Significantly enriched KEGG pathways based on 3′ Tag-seq in primary mammary tumors from PyMT hemizygous female mice with either (*D*) methylparaben or (*E*) propylparaben exposure relative to the vehicle control. Gradient scale represents the number of genes in the KEGG pathway and the number above the bar represents the number of genes detected in the mammary tumors within the KEGG pathway. $*P<0.05$, $**P<0.01$, $***P<0.001$ relative to the vehicle control with mean and standard error graphed for 19-20 mice/treatment.

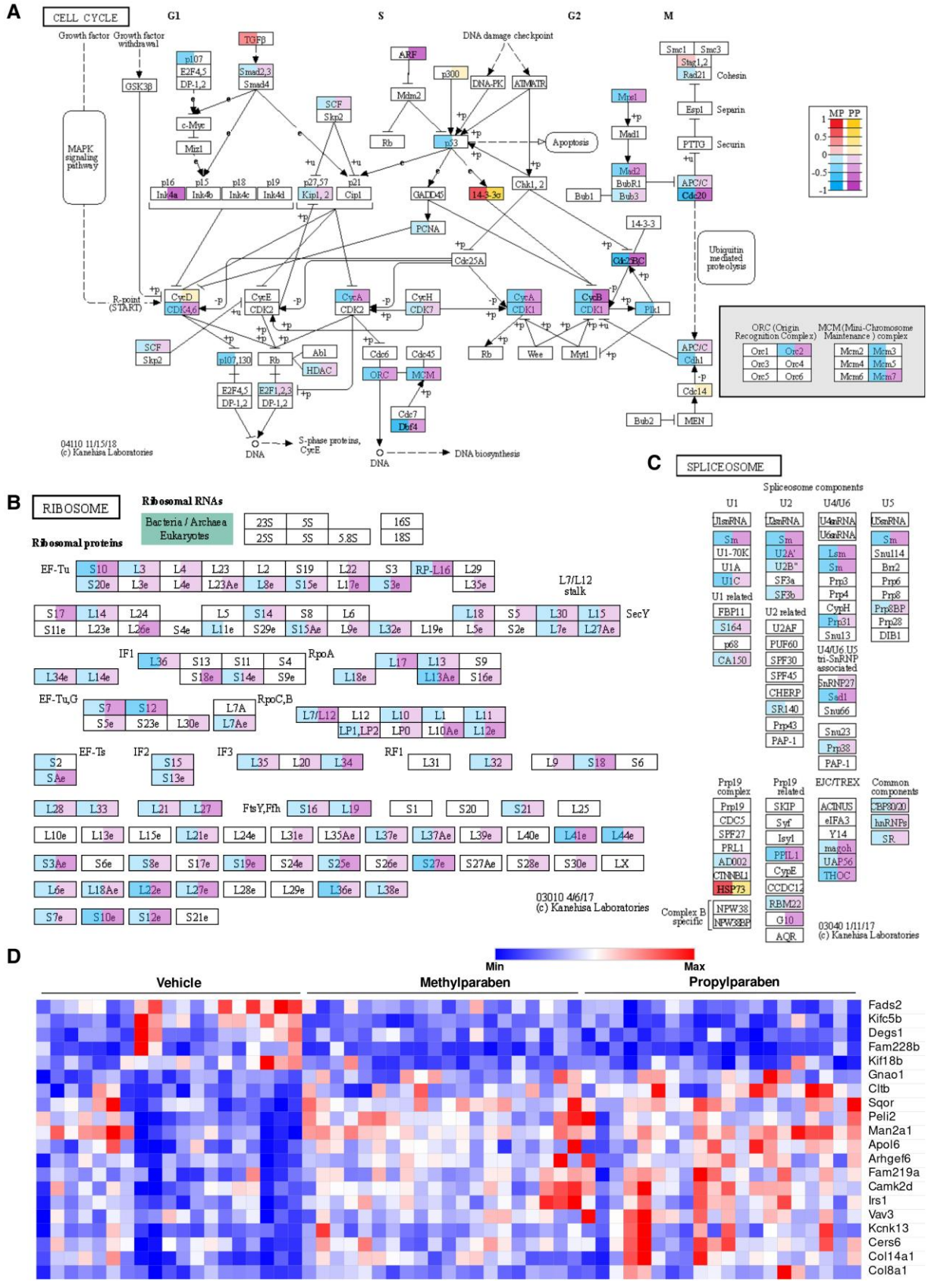

Figure 5. Parabens and RNA metabolism in primary mammary tumors. (*A-C*) Top common KEGG pathways in primary mammary tumors from PyMT hemizygous female mice enriched by methylparaben (MP) and propylparaben (PP) treatment relative to the vehicle control (VEH); (*A*) cell cycle, (*B*) ribosome, and (*C*) spliceosome. Gradient scale represents increased or decreased fold expression in MP vs VEH or PP vs VEH. (*D*) Heat map of the 20 genes that were significantly enriched with intronic RNA (normalized counts per tumor) in PyMT hemizygous female mice treated with PP relative to VEH. Gradient scale represents relative amount of intron counts.

LBD structure and residue contacts with both E2 and parabens (65). Instead, it may be that paraben alkyl chain length influences ER transactivation through altered allosteric regulation of ER and/or mobility of the paraben-ER complex (55, 66-68).

Several lines of evidence suggest that paraben activation of ER may not be the sole mechanism of paraben carcinogenesis (61, 63). For example, numerous studies have indicated that the shortest alkyl chain length paraben, MP, is a very weak activator of (16, 20, 21) or even inactive at (22, 23) ER, which is inconsistent with the elevated mammary TEB abundance, tumor growth, and metastasis we observed in mice exposed to MP at levels relevant to humans. Although paraben-stimulated ER signaling could have promoted tumor growth, ER pathways may not be required, or may be augmented by secondary gene alterations (57, 69). This is consistent with the lack of effect of either paraben on *c-Myc* or *Cyclin D1* expression and the lack of enrichment of the KEGG Estrogen Signaling pathway by parabens in mammary tumors here. Hence, the mechanism of paraben effects on cancer likely extends beyond agonism of ER.

Several lines of evidence indicate that abnormal splicing by parabens may also contribute to the increased rates of metastasis they caused (70). For example, engineered modulation of spliceosome gene expression increased intron retention and metastasis of human breast cancer cells in vivo, and reduced spliceosome expression in primary breast tumors was associated with reduced metastasis-free survival (71, 72). Indeed, several studies have associated alternative splicing with pulmonary metastasis of breast cancer and decreased breast cancer survival (70, 73, 74). Additionally, the increased mammary tumor growth rate by parabens is consistent with the substantially reduced tumor growth of mice treated with a spliceosome inhibitor (75).

Two of the top 3 genes with differentially expressed introns, *Fads2* and *Degs1*, are lipid desaturases for which activity can lead to proliferation in cancer (76). Delta-6 desaturase, encoded by *Fads2*, is involved in polyunsaturated fatty acid elongation, beta-oxidation, and tumor metabolic plasticity (77, 78). Consistent with a functional role of parabens in fatty acid metabolism, both MP and PP have been associated with acylcarnitines in the urine of women and reduced basal lipolysis in adipocytes (24, 79). *Fads2* may link these parabens with mammary cancer metastasis given *Fads2* had the lowest expression in breast cancer patients with poor prognosis and/or who died (80). Further, alternative splicing of *Fads2* (and 2 genes with enriched intron retention by PP: *Arhgef6*, *Cers6*) was significantly associated with overall breast cancer (Triple-Negative Breast Cancer [TNBC]) survival in The Cancer Genome Atlas SpliceSeq database https://bioinformatics.mdanderson.org/TCGASpliceSeq/ (81).

One strength of this study was the selected mouse model (82). Many characteristics of the mammary tumors in PyMT mice are shared with breast cancer in humans (83). Importantly, this is one of the few mouse models of human breast cancer that spontaneously metastasizes (82), a significant cause of breast cancer mortality because breasts are non-vital organs. One limitation of this study was the detection of MP in the mice from the VEH group. Although the MP detected in mice assigned to the VEH group was 3155-fold lower than that detected in the mice assigned to paraben exposure, it could have biased our estimates of paraben effects toward the null. Another limitation is that our estimates of intron expression are likely underreported given the library preparation is complementary to 3′ end sequences. These limitations would mean that the true paraben effects could be larger than reported here.

We show that paraben exposure at levels common in the US population are capable of accelerating mammary cancer growth and metastasis in mice through at least 2 key characteristics of carcinogens (58) and alternative splicing events (72). These data support the provocative possibility that disproportionate paraben exposure is related to the disproportionate risk of ER+/luminal breast cancer mortality among Black women (9-12, 84). Unfortunately, regulatory toxicology test guidelines for carcinogenicity are inadequately designed to replicate our findings and the logistical challenges preclude rapid confirmation of whether our results would extend to human breast cancer (eg, decades of exposure assessment, outcome follow-up) (85). The FDA should consider reevaluating the "human acceptable daily intake" of these chemicals and consumers may wish to reexamine their personal care product use (86).

Acknowledgments

We would like to thank Dr. Robert Cardiff and the UC Davis Department of Pathology and Laboratory Medicine for assisting in histopathology analyses our animal tissues. We also offer a post mortem acknowledgment to Dr. Michael Denison for his guidance on the luciferase assays and providing those cells. Raw and processed RNA-sequencing data of primary mammary tumors were deposited in the GEO database under accession number GSE175625.

Funding

This work was supported by Office of Environmental Health Hazard Assessment of the California Environmental Protection Agency (17-E0024); USDA National Institute of Food and Agriculture (1002182); and National Institutes of Health (R42-ES004699).

Disclosures

The authors have nothing to disclose.

Data Availability

Some or all datasets generated during and/or analyzed during the current study are not publicly available but are available from the corresponding author on reasonable request.

References

1. Andersen FA. Final amended report on the safety assessment of methylparaben, ethylparaben, propylparaben, isopropylparaben, butylparaben, isobutylparaben, and benzylparaben as used in cosmetic products. *Int J Toxicol*. 2008;27(4_suppl):1-82.
2. Darbre PD, Harvey PW. Paraben esters: review of recent studies of endocrine toxicity, absorption, esterase and human exposure, and discussion of potential human health risks. *J Appl Toxicol*. 2008;28(5):561-578.
3. Nowak K, Ratajczak–Wrona W, Gorska M, Jabłońska E. Parabens and their effects on the endocrine system. *Mol Cell Endocrinol*. 2018;474:238-251.

4. Artacho-Cordón F, Fernández M, Frederiksen H, *et al.* Environmental phenols and parabens in adipose tissue from hospitalized adults in southern Spain. *Environ Int*. 2018;119:203-211.
5. Azzouz A, Rascón AJ, Ballesteros E. Simultaneous determination of parabens, alkylphenols, phenylphenols, bisphenol A and triclosan in human urine, blood and breast milk by continuous solid-phase extraction and gas chromatography–mass spectrometry. *J Pharm Biomed Anal*. 2016;119:16-26.
6. Darbre PD, Aljarrah A, Miller WR, Coldham NG, Sauer MJ, Pope G. Concentrations of parabens in human breast tumours. *J Appl Toxicol*. 2004;24(1):5-13.
7. Frederiksen H, Jørgensen N, Andersson A-M. Parabens in urine, serum and seminal plasma from healthy Danish men determined by liquid chromatography–tandem mass spectrometry (LC–MS/MS). *J Expo Sci Environ Epidemiol*. 2011;21(3):262-271.
8. Quirós-Alcalá L, Buckley JP, Boyle M. Parabens and measures of adiposity among adults and children from the US general population: NHANES 2007–2014. *Int J Hyg Environ Health*. 2018;221(4):652-660.
9. Buttke DE, Sircar K, Martin C. Exposures to endocrine-disrupting chemicals and age of menarche in adolescent girls in NHANES (2003–2008). *Environ Health Perspect*. 2012;120(11):1613-1618.
10. Nguyen VK, Kahana A, Heidt J, *et al.* A comprehensive analysis of racial disparities in chemical biomarker concentrations in United States women, 1999–2014. *Environ Int*. 2020;137:105496.
11. O'Brien C, Wallin JJ, Sampath D, *et al.* Predictive biomarkers of sensitivity to the phosphatidylinositol 3′ kinase inhibitor GDC-0941 in breast cancer preclinical models. *Clin Cancer Res*. 2010;16(14):3670-3683.
12. Benefield HC, Reeder-Hayes KE, Nichols HB, *et al.* Outcomes of hormone-receptor positive, HER2-negative breast cancers by race and tumor biological features. *JNCI Cancer Spectrum*. 2021;5(1):pkaa072.
13. Byford J, Shaw L, Drew M, Pope G, Sauer M, Darbre P. Oestrogenic activity of parabens in MCF7 human breast cancer cells. *J Steroid Biochem Mol Biol*. 2002;80(1):49-60.
14. Darbre P, Byford J, Shaw L, Horton R, Pope G, Sauer M. Oestrogenic activity of isobutylparaben in vitro and in vivo. *J Appl Toxicol*. 2002;22(4):219-226.
15. Khanna S, Darbre PD. Parabens enable suspension growth of MCF-10A immortalized, non-transformed human breast epithelial cells. *J Appl Toxicol*. 2013;33(5):378-382.
16. Okubo T, Yokoyama Y, Kano K, Kano I. ER-dependent estrogenic activity of parabens assessed by proliferation of human breast cancer MCF-7 cells and expression of ERα and PR. *Food Chem Toxicol*. 2001;39(12):1225-1232.
17. Pop A, Drugan T, Gutleb AC, *et al.* Estrogenic and anti-estrogenic activity of butylparaben, butylated hydroxyanisole, butylated hydroxytoluene and propyl gallate and their binary mixtures on two estrogen responsive cell lines (T47D-Kbluc, MCF-7). *J Appl Toxicol*. 2018;38(7):944-957.
18. Khanna S, Dash PR, Darbre PD. Exposure to parabens at the concentration of maximal proliferative response increases migratory and invasive activity of human breast cancer cells in vitro. *J Appl Toxicol*. 2014;34(9):1051-1059.
19. Hanahan D, Weinberg RA. Hallmarks of cancer: the next generation. *Cell*. 2011;144(5):646-674.
20. Charles AK, Darbre PD. Combinations of parabens at concentrations measured in human breast tissue can increase proliferation of MCF-7 human breast cancer cells. *J Appl Toxicol*. 2013;33(5):390-398.
21. Gomez E, Pillon A, Fenet H, *et al.* Estrogenic activity of cosmetic components in reporter cell lines: parabens, UV screens, and musks. *J Toxicol Environ Health, Part A*. 2005;68(4):239-251.
22. Lillo MA, Nichols C, Perry C, *et al.* Methylparaben stimulates tumor initiating cells in ER+ breast cancer models. *J Appl Toxicol*. 2017;37(4):417-425.
23. Terasaka S, Inoue A, Tanji M, Kiyama R. Expression profiling of estrogen-responsive genes in breast cancer cells treated with alkylphenols, chlorinated phenols, parabens, or bis-and benzoylphenols for evaluation of estrogenic activity. *Toxicol Lett*. 2006;163(2):130-141.
24. Elmore S, Cano-Sancho G, La Merrill M. Disruption of normal adipocyte development and function by methyl-and propyl-paraben exposure. *Toxicol Lett*. 2020;334:27-35.
25. Hu P, Chen X, Whitener RJ, *et al.* Effects of parabens on adipocyte differentiation. *Toxicol Sci*. 2013;131(1):56-70.
26. Taxvig C, Dreisig K, Boberg J, *et al.* Differential effects of environmental chemicals and food contaminants on adipogenesis, biomarker release and PPARγ activation. *Mol Cell Endocrinol*. 2012;361(1-2):106-115.
27. Hu P, Kennedy RC, Chen X, *et al.* Differential effects on adiposity and serum marker of bone formation by post-weaning exposure to methylparaben and butylparaben. *Environ Sci Pollut Res*. 2016;23(21):21957-21968.
28. Leppert B, Strunz S, Seiwert B, *et al.* Maternal paraben exposure triggers childhood overweight development. *Nat Commun*. 2020;11(1):561.
29. Peto J. Cancer epidemiology in the last century and the next decade. *Nature*. 2001;411(6835):390-395.
30. Gopalakrishnan K, Teitelbaum SL, Lambertini L, *et al.* Changes in mammary histology and transcriptome profiles by low-dose exposure to environmental phenols at critical windows of development. *Environ Res*. 2017;152:233-243.
31. Tong JH, Elmore S, Huang S-S, *et al.* Data from: Chronic exposure to low levels of parabens increases mammary cancer growth and metastasis in mice. Deposited January 6, 2023. https://doi.org/10.6084/m9.figshare.21834441.
32. Namba R, Young LJ, Maglione JE, *et al.* Selective estrogen receptor modulators inhibit growth and progression of premalignant lesions in a mouse model of ductal carcinoma in situ. *Breast Cancer Res*. 2005;7(6):1-9.
33. Guy CT, Cardiff R, Muller WJ. Induction of mammary tumors by expression of polyomavirus middle T oncogene: a transgenic mouse model for metastatic disease. *Mol Cell Biol*. 1992;12(3):954-961.
34. Maglione JE, McGoldrick ET, Young LJ, *et al.* Polyomavirus middle T–induced mammary intraepithelial neoplasia outgrowths: single origin, divergent evolution, and multiple outcomes. *Mol Cancer Ther*. 2004;3(8):941-953.
35. Qiu TH, Chandramouli GV, Hunter KW, Alkharouf NW, Green JE, Liu ET. Global expression profiling identifies signatures of tumor virulence in MMTV-PyMT-transgenic mice: correlation to human disease. *Cancer Res*. 2004;64(17):5973-5981.
36. Davie SA, Maglione JE, Manner CK, *et al.* Effects of FVB/NJ and C57Bl/6J strain backgrounds on mammary tumor phenotype in inducible nitric oxide synthase deficient mice. *Transgenic Res*. 2007;16(2):193-201.
37. Ellies LG, Fishman M, Hardison J, *et al.* Mammary tumor latency is increased in mice lacking the inducible nitric oxide synthase. *Int J Cancer*. 2003;106(1):1-7.
38. Matouskova K, Szabo GK, Daum J, *et al.* Best practices to quantify the impact of reproductive toxicants on development, function, and diseases of the rodent mammary gland. *Reproductive Toxicol*. 2022;112:51-67.
39. Mori H, Chen JQ, Cardiff RD, *et al.* Pathobiology of the 129: Stat1 −/− mouse model of human age-related ER-positive breast cancer with an immune infiltrate-excluded phenotype. *Breast Cancer Res*. 2017;19(1):1-18.
40. La Merrill M, Harper R, Birnbaum LS, Cardiff RD, Threadgill DW. Maternal dioxin exposure combined with a diet high in fat increases mammary cancer incidence in mice. *Environ Health Perspect*. 2010;118(5):596-601.
41. Miller JW, Borowsky AD, Marple TC, *et al.* DNA methylation, and mouse models of breast tumorigenesis. *Nutr Rev*. 2008;66(suppl_1):S59-S64.
42. Bankhead P, Loughrey MB, Fernández JA, *et al.* Qupath: open source software for digital pathology image analysis. *Sci Rep*. 2017;7(1):1-7.

43. Aubert N, Ameller T, Legrand J-J. Systemic exposure to parabens: pharmacokinetics, tissue distribution, excretion balance and plasma metabolites of [14C]-methyl-, propyl-and butylparaben in rats after oral, topical or subcutaneous administration. *Food Chem Toxicol*. 2012;50(3-4):445-454.
44. Tahan GP, Santos NDKS, Albuquerque AC, Martins I. Determination of parabens in serum by liquid chromatography-tandem mass spectrometry: correlation with lipstick use. *Regul Toxicol Pharmacol*. 2016;79:42-48.
45. Tachachartvanich P, Sangsuwan R, Ruiz HS, *et al.* Assessment of the endocrine-disrupting effects of trichloroethylene and its metabolites using in vitro and in silico approaches. *Environ Sci Technol*. 2018;52(3):1542-1550.
46. Brennan JC, Bassal A, He G, Denison MS. Development of a recombinant human ovarian (BG1) cell line containing estrogen receptor α and β for improved detection of estrogenic/antiestrogenic chemicals. *Environ ToxicolChem* 2016;35(1):91-100.
47. Law CW, Chen Y, Shi W. Smyth GK. Voom: precision weights unlock linear model analysis tools for RNA-seq read counts. *Genome Biol*. 2014;15(2):1-17.
48. Kanehisa M, Goto S. KEGG: Kyoto Encyclopedia of Genes and Genomes. *Nucleic Acids Res*. 2000;28(1):27-30.
49. Tenenbaum D. KEGGREST: Client-side REST access to KEGG. *R package version* 1181. 2020;1(1).
50. Luo W, Brouwer C. Pathview: an R/bioconductor package for pathway-based data integration and visualization. *Bioinformatics*. 2013;29(14):1830-1831.
51. Joint FAO/WHO Expert Committee on Food Additives, Organization WH. Toxicological evaluation of certain food additives with a review of general principles and of specifications: seventeenth report of the Joint FAO/WHO Expert Committee on Food Additives, Geneva, 25 June-4 July 1973. World Health Organization.
52. Reagan-Shaw S, Nihal M, Ahmad N. Dose translation from animal to human studies revisited. *FASEB J*. 2008;22(3):659-661.
53. Toxicological evaluation of certain food additives with a review of general principles and of specifications: seventeenth report of the Joint FAO/WHO Expert Committee on Food Additives, Geneva, 25 June-4 July 1973. World Health Organization; 1974.
54. JECFA. Toxicological evaluation of certain food additives with a review of general principles and of specifications: seventeenth report of the Joint FAO/WHO Expert Committee on Food Additives, Geneva, 25 June-4 July 1973. World Health Organization.
55. Smith LC, Clark JC, Bisesi Jr JH, Ferguson PL, Sabo-Attwood T. Differential recruitment of co-regulatory proteins to the human estrogen receptor 1 in response to xenoestrogens. *Comp Biochem Physiol Part D: Genomics Proteomics*. 2016;19:159-173.
56. Cosphiadi I, Atmakusumah TD, Siregar NC, Muthalib A, Harahap A, Mansyur M. Bone metastasis in advanced breast cancer: analysis of gene expression microarray. *Clin Breast Cancer*. 2018;18(5): e1117-e1122.
57. Lei JT, Gou X, Seker S, Ellis MJ. ESR1 alterations and metastasis in estrogen receptor positive breast cancer. *J Cancer Metastasis Treatment*. 2019;5:38.
58. Smith MT, Guyton KZ, Gibbons CF, *et al.* Key characteristics of carcinogens as a basis for organizing data on mechanisms of carcinogenesis. *Environ Health Perspect*. 2016;124(6):713-721.
59. Dairkee SH, Luciani-Torres G, Moore DH, Jaffee IM, Goodson III WH. A ternary mixture of common chemicals perturbs benign human breast epithelial cells more than the same chemicals do individually. *Toxicol Sci*. 2018; 165(1):131-144.
60. Mogus JP, LaPlante CD, Bansal R, *et al.* Exposure to propylparaben during pregnancy and lactation induces long-term alterations to the mammary gland in mice. *Endocrinology*. 2021;162(6): bqab041.
61. Darbre PD, Harvey PW. Parabens can enable hallmarks and characteristics of cancer in human breast epithelial cells: a review of the literature with reference to new exposure data and regulatory status. *J Appl Toxicol*. 2014;34(9):925-938.
62. Aushev VN, Gopalakrishnan K, Teitelbaum SL, *et al.* Tumor expression of environmental chemical-responsive genes and breast cancer mortality. *Endocr Relat Cancer*. 2019;26(12):843-851.
63. Marchese S, Silva E. Disruption of 3D MCF-12A breast cell cultures by estrogens–an in vitro model for ER-mediated changes indicative of hormonal carcinogenesis. *PloS One*. 2012;7(10):e45767.
64. Nair S, Sachdeva G. Estrogen matters in metastasis. *Steroids*. 2018;138:108-116.
65. Gonzalez TL, Rae JM, Colacino JA, Richardson RJ. Homology models of mouse and rat estrogen receptor-α ligand-binding domain created by in silico mutagenesis of a human template: molecular docking with 17β-estradiol, diethylstilbestrol, and paraben analogs. *Comput Toxicol*. 2019;10:1-16.
66. Brzozowski AM, Pike AC, Dauter Z, *et al.* Molecular basis of agonism and antagonism in the oestrogen receptor. *Nature*. 1997; 389(6652):753-758.
67. Xue Q, Liu X, Liu X-C, Pan W-X, Fu J-J, Zhang A-Q. The effect of structural diversity on ligand specificity and resulting signaling differences of estrogen receptor α. *Chem Res Toxicol*. 2019;32(6): 1002-1013.
68. Xue Q, Liu X, Liu XC, Pan WX, Fu JJ, Zhang AQ. The effect of structural diversity on ligand specificity and resulting signaling differences of estrogen receptor alpha. *Chem Res Toxicol*. 2019;32(6): 1002-1013.
69. Klebe M, Fremd C, Kriegsmann M, *et al.* Frequent molecular subtype switching and gene expression alterations in lung and pleural metastasis from luminal A–type breast cancer. *JCO Precision Oncol*. 2020;4(4):848-859.
70. Fish L, Khoroshkin M, Navickas A, *et al.* A prometastatic splicing program regulated by SNRPA1 interactions with structured RNA elements. *Science*. 2021;372(6543):eabc7531.
71. An J, Luo Z, An W, Cao D, Ma J, Liu Z. Identification of spliceosome components pivotal to breast cancer survival. *RNA Biol*. 2020;18(6):833-842.
72. Nguyen A, Yoshida M, Goodarzi H, Tavazoie SF. Highly variable cancer subpopulations that exhibit enhanced transcriptome variability and metastatic fitness. *Nat Commun*. 2016;7(1):1-13.
73. Gökmen-Polar Y, Neelamraju Y, Goswami CP, *et al.* Expression levels of SF3B3 correlate with prognosis and endocrine resistance in estrogen receptor-positive breast cancer. *Mod Pathol*. 2015;28(5):677-685.
74. Wu J, Yang T, Lu P, Ma W. Analysis of signaling pathways in recurrent breast cancer. *Genet Mol Res*. 2014;13(4):10097-10104.
75. Huang HH, Ferguson ID, Thornton AM, *et al.* Proteasome inhibitor-induced modulation reveals the spliceosome as a specific therapeutic vulnerability in multiple myeloma. *Nat Commun*. 2020;11(1):1-14.
76. Berquin IM, Edwards IJ, Kridel SJ, Chen YQ. Polyunsaturated fatty acid metabolism in prostate cancer. *Cancer Metastasis Rev*. 2011;30(3-4):295-309.
77. Cho HP, Nakamura MT, Clarke SD. Cloning, expression, and nutritional regulation of the mammalian Δ-6 desaturase. *JBiol Chem*. 1999;274(1):471-477.
78. Vriens K, Christen S, Parik S, *et al.* Evidence for an alternative fatty acid desaturation pathway increasing cancer plasticity. *Nature*. 2019;566(7744):403-406.
79. Zhao H, Zheng Y, Zhu L, *et al.* Paraben exposure related to purine metabolism and other pathways revealed by mass spectrometry-based metabolomics. *Environ Sci Technol*. 2020;54(6):3447-3454.
80. Lane J, Mansel RE, Jiang WG. Expression of human delta-6-desaturase is associated with aggressiveness of human breast cancer. *Int J Mol Med*. 2003;12(2):253-257.
81. Gong S, Song Z, Spezia-Lindner D, *et al.* Novel insights into triple-negative breast cancer prognosis by comprehensive characterization of aberrant alternative splicing. *Front Genet*. 2020;11:534.

82. Lin EY, Jones JG, Li P, *et al*. Progression to malignancy in the polyoma middle T oncoprotein mouse breast cancer model provides a reliable model for human diseases. *Am J Pathol*. 2003;163(5):2113-2126.
83. Fantozzi A, Christofori G. Mouse models of breast cancer metastasis. *Breast Cancer Res*. 2006;8(4):212.
84. Pellom ST, Arnold T, Williams M, Brown VL, Samuels AD. Examining breast cancer disparities in African Americans with suggestions for policy. *Cancer Causes Control*. 2020;31:795-800.
85. Kay JE, Cardona B, Rudel RA, *et al*. Chemical effects on breast development, function, and cancer risk: existing knowledge and new opportunities. *Curr Environ Health Rep*. 2022;9(4):535-562.
86. Harley KG, Kogut K, Madrigal DS, *et al*. Reducing phthalate, paraben, and phenol exposure from personal care products in adolescent girls: findings from the HERMOSA intervention study. *Environ Health Perspect*. 2016;124(10):1600-1607.